Primary Cosmic Ray Flux

Todor Stanev[a]

[a]Bartol Research Institute, University of Delaware,
Newark, DE 19716, U.S.A.

We discuss the primary cosmic ray flux from the point of view of particle interactions and production of atmospheric neutrinos. The overall normalization of the cosmic ray flux and its time variations and site dependence are major ingredients of the atmospheric neutrino predictions and the basis for the derivation of the neutrino oscillation parameters.

1. INTRODUCTION

We discuss the primary cosmic ray flux from the point of view of production and detection of atmospheric neutrinos. These neutrinos are generated in the decay chain of mesons and muons, generated in atmospheric cascades initiated by primary cosmic ray interactions in the atmosphere. Because of the weak interaction cross section of neutrinos it is unlikely that two neutrinos generated in the same cascade will be ever detected by an experiment. Atmospheric neutrino flux is thus flux of uncorrelated particles. The flux of such particles can be calculated [1] under the assumption that treats treats every constituent nucleon of the primary cosmic ray nuclei as a free nucleon. The flux of cosmic ray nucleons is dominated by protons (hydrogen nuclei) and helium. At kinetic energy of 10.6 GeV hydrogen contributes [2] 75% of all nucleons and helium contributes another 16%. The rest comes from heavier cosmic ray nuclei. The good knowledge of the hydrogen and helium fluxes is extremely important for a good prediction of the atmospheric neutrinos.

Experimentally there are several types of events:
1) Fully contained (FC) events, where both the interaction vertex and the whole event track are contained in the fiducial volume of the detector. The Super–Kamiokande collaboration has a sub-classification of sub–GeV and multi–GeV FC events.
2) Partially contained (PC) events, where the interaction vertex is contained in the fiducial volume, but a part of the track is outside.
3) Upward going muons, where the interaction vertex is outside the detector and only the generated muon enters the detector from below. The shielding of the detector by the Earth insures that only neutrino generated muons could penetrate the detector from below. Upward going muons are usually subdivided into throughgoing and stopping.

These classes of events correspond to different neutrino energy ranges and correspondingly neutrino cross sections. The sub–GeV FC events detected by Super–Kamiokande are generated by quasielastic interactions of neutrinos of average energy just below 1 GeV. The response for multi–GeV FC events and PC events peaks at several GeV, depending on the detector design and experimental cuts, and involves quasielastic, 1–pion and deep inelastic interactions. The response for stopping upward going muons is quite similar. Finally, upward going throughgoing muons are generated by a wide spectrum of neutrinos, peaking at about 100 GeV and extending to more than 1000 GeV. Knowing the neutrino spectra that generate the different experimental events one can estimate the corresponding primary cosmic ray flux ranges. These are shown in Fig. 1 with bands that extend from 5% to 95% of the signals.

2. NORMALIZATION OF THE PRIMARY COSMIC RAY FLUX

Until several years ago the normalization of the primary cosmic ray flux below 100 GeV was a major uncertainty in the prediction of atmospheric neutrinos. There were generally two different normalizations: high, coming from the 1977–79 data of Webber et al [3] and low, introduced by the LEAP experiment [4]. The experiments of 1990s [5–7] all agreed better with the low normalization. All these data sets were obtained with magnetic spectrometers, involving different experimental arrangements working with the New Mexico State superconducting magnet. The breakthrough came this year, when two entirely new experiments, AMS [8,9] and BESS [10] with respectively different systematics, published hydrogen and helium spectra very similar to each other's.

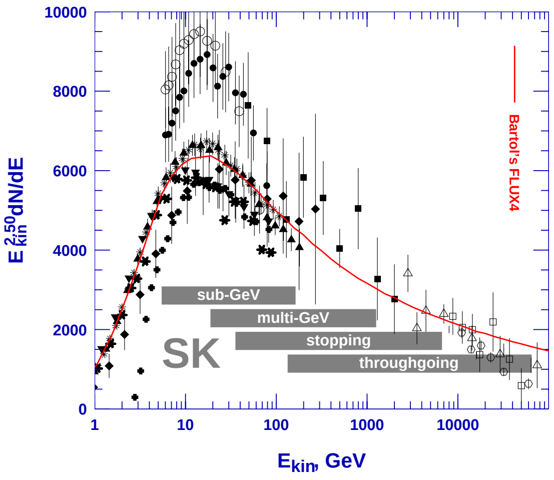

Figure 1. Comparison of different data sets on the cosmic ray flux of hydrogen to the model used by the Bartol group for predictions of atmospheric neutrinos. Flux units are m^{-2} s^{-1}ster^{-1}GeV$^{1.5}$. The bands show the energy ranges responsible for 90% of the neutrino events in the Super–Kamiokande detector.

Fig. 1 shows all these experimental data sets for hydrogen. The data of AMS are shown with full triangles and those of BESS - with asterisks. These two data sets are practically on top of each other. If one measures the difference between them as $\Delta = 2(F_1 - F_2)/(F_1 + F_2)$ the average Δ value is 1.7%, less than the average uncertainty of each of the data sets which is around 4%. The experimental errors are dominated by systematic errors. In the 10 – 30 GeV region, which is most important for the FC neutrino events, the new data sets are about 10% higher than the other relatively recent measurements. The line in Fig. 1 shows the primary proton spectrum used for prediction of the atmospheric neutrino flux by the Bartol group [11]. In the energy range responsible for the contained neutrino events it is in very good agreement with the new measurements, in spite of the incorrect statement in Ref. [8]. The agreement in the new helium data sets is not as good as for the hydrogen fluxes, although it is still at an acceptable level . Flux models used for atmospheric neutrino predictions have to be corrected in full agreement with the new data sets, but the contribution of the primary flux normalization to the predictions for contained neutrino events is now significantly lower than 10%.

This is not true for the whole neutrino energy range. Above 200 GeV or so the experimental data becomes very scarce and uncertain. Most of the statistics is above 1 TeV and comes from balloon emulsion chamber experiments [12,13]. These experiments measure the cosmic ray energy by the electromagnetic energy of the particle interaction in the detector ΣE_γ. On top of the usual statistical and systematic uncertainties, this technique also suffers from the fluctuations in the fraction of the neutral secondaries in inelastic hadronic interactions, as well as from the possible energy leakage from the thin calorimeters that these detectors can afford to fly. The uncertainty at energies above 100 GeV is thus much higher.

3. SOLAR MODULATION

It has been well known for many years now that the flux of galactic cosmic rays varies with the epoch of the solar cycle. The reason is that charged cosmic rays scatter on the magnetic field

frozen in the solar wind. Cosmic rays propagating in the solar wind are subject to:
1) diffusion through the turbulent magnetic field,
2) convection due to the outward motion of the field, and
3) adiabatic energy loss.
All three processes depend on the strength of the solar wind and the embedded magnetic field and the cosmic ray flux is inversely proportional to the sunspot number with a timelag of about one year, close to the propagation time of the solar wind to the boundary of the heliosphere. The simplest way to relate the local (in the vicinity of the Earth) and interstellar cosmic ray fluxes is through the force field solution [14] of the propagation equation that expresses the energy loss and loss of particle flux in terms of a single *modulation parameter* Φ. The local cosmic rays flux $J(E)$ is related to the interstellar flux J_{IS} as

$$J(E) \;=\; \frac{E^2 - m^2}{(E+\Phi)^2 - m^2} J_{IS}(E+\Phi)\;, \qquad (1)$$

where E is the total particle energy and m is the particle mass. This formula does not work well at very low energies, but seems to be sufficiently good at kinetic energies above a couple of GeV. It is important to note that the anisotropy due to the convection is small in the vicinity of the Earth - it is estimated to be about 0.5% for particles of energy from 1 to 100 GeV [15].

Experimentally the solar modulation is studied mostly with neutron monitors, surface detectors that integrate over the flux between several and several hundred GeV. The cosmic ray response to the neutron monitor counts is fortunately very close to that of contained neutrino events. Fig. 2 shows the monthly averages of the neutron monitor counts at moderate geomagnetic latitude. The way most of the neutrino predictions are normalized now is through the cosmic ray fluxes at two arbitrarily chosen epochs that we usually call solar maximum and solar minimum. These are represented with two bands in Fig. 1. It is obvious from the figure, however, that the true flux values vary in magnitude and in periodicity. The correct way for dealing with this time dependence is to integrate the cosmic ray flux for the duration of the experiment. This could be done by the introduction of a standard interstellar cosmic ray spectrum and accounting for the solar modulation with modulation parameters estimated from the neutron monitor counts at different geomagnetic latitudes.

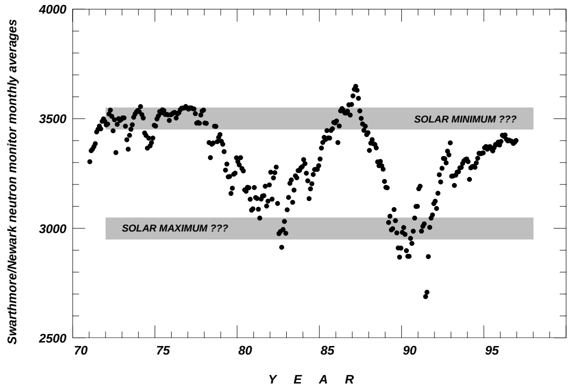

Figure 2. Monthly average counts of the Swarthmore/Newark neutron monitor. The flux of vertically downgoing GeV neutrinos would have similar time variation. The bands show the arbitrarily chosen epochs of solar maximum and solar minimum.

4. GEOMAGNETIC EFFECTS

Cosmic rays also scatter on the geomagnetic field prior to their interactions in the atmosphere and during the shower development. One of the consequences is that some low energy cosmic rays cannot propagate deeply enough, interact and initiate atmospheric cascades. For historical reasons this effect is called *geomagnetic cutoff* although for any angular range it could be better described as a propagation efficiency that has 0 value at very low rigidity (momentum per charge) and gradually increases to 1 at some higher rigidity R_{GM}. The energy dependence of the propagation efficiency and the R_{GM} value depend on the geomagnetic latitude and the angle between the cosmic ray direction and the geomagnetic field lines.

The geomagnetic field is generally an offset dipole field with a magnetic South pole at latitude of 81° and longitude of 84.7°W, i.e. currently the geomagnetic field lines flow from South to North. In the case of purely dipole field the propagation in the geomagnetic field can be solved so that there is indeed a step function, a cutoff rigidity R_S (derived by Störmer) under which cosmic ray particles cannot arrive at certain altitude, angle and geomagnetic latitude. The maximum cutoff rigidity is 59 GV, at which the charged particles orbit the Earth around the geomagnetic equator.

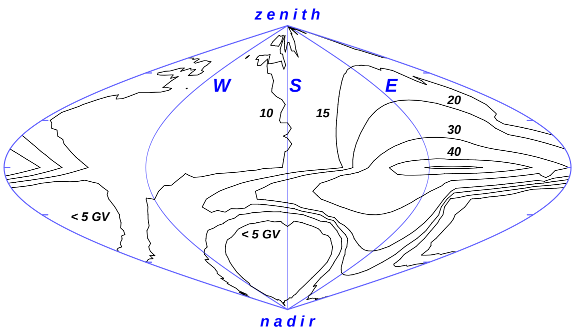

Figure 3. Geomagnetic cutoff map for the location of Super–Kamiokande. Note the location of the two geomagnetic poles and the very high geomagnetic cutoffs in Eastern direction around the horizon.

The geomagnetic field is very well known, monitored and updated [16]. The most convenient way to study charged particle propagations is to 'backtrack' antiprotons injected with certain angle at certain location and altitude. If these antiprotons can reach a 'safe' distance from the Earth, where cosmic rays are practically isotropic, then the primary cosmic rays can reach the same altitude and interact there to produce secondaries and initiate an atmospheric cascade. Antiprotons that do not reach that distance are either trapped in the geomagnetic field or 'shadowed' by the Earth itself.

Fig. 3 shows the geomagnetic cutoff map for the location of Super–Kamiokande. The top of the map corresponds to the zenith and the geographic directions are indicated, except that North is split between the extreme left and right. One can easily detect the directions of the two geomagnetic poles where the cutoff is less than 5 GV. The highest cutoffs are in Eastern direction where there is a small solid angle with a cutoff above 50 GV. The general situation seen in the map is that the geomagnetic cutoffs above the horizon are higher than below the horizon.

The angular distribution of the sub–GeV fully contained events in Super–Kamiokande is to a large extent determined by this map (except for the geometry of the neutrino production in the atmosphere [17]). It also determines the East–West effect in atmospheric neutrinos detected by Super–Kamiokande [18]. It is due to the fact that cosmic rays, being positively charged, reach the atmosphere much easier from the West than from the East. This generates higher neutrino flux from the West [19,20].

Soudan 2 and SNO are, on the contrary, located very close to the geomagnetic pole where the geomagnetic cutoffs are very low. One has to realize that the fluxes of downgoing neutrinos reflect the geomagnetic conditions at the site of the experiment while for the fluxes of upgoing neutrinos one has to integrate over the whole surface of the Earth. Thus in Soudan 2 and SNO one has to expect more downgoing than upgoing neutrinos, opposite to the situation at Super–Kamiokande.

5. ATMOSPHERIC NEUTRINOS VS COSMIC RAYS

As nicely the Super–Kamiokande data [21] are explained by $\nu_\mu \to \nu_\tau$ oscillations there have been recently several reasons for which we ought to challenge the predictions of the atmospheric neutrino flux. One of them is the absolute normalization of the flux of electron–like events, which is 9% higher than predicted at Super–K and 21% lower than predicted at Soudan 2. This is a contradiction that cannot be explained by the statistical uncertainty of the Soudan 2 data.

Another worry comes from the new developments in the atmospheric neutrino calculations. The 3D calculation with the sophisticated and very well tested with accelerator data code FLUKA [22] shows uniformly about 20% less neutrinos than the Bartol calculation [11]. The same primary spectrum is used in both calculations and the difference is not due to the low energy 3D effects [23]. The question how well we understand the data on atmospheric neutrinos is again relevant and we have to answer it on a better than 20% level.

These questions are even more important for the higher energy neutrinos that generate upward going muons.

5.1. Solar modulation of the atmospheric neutrino flux

Fig. 4 shows the cosmic ray response to sub–GeV fully contained events (using Super–K definition) at the locations of Kamioka and Soudan 2/SNO. At high geomagnetic latitude the cosmic ray response peaks just below 10 GeV, while at Kamioka the peak is at about 15 GeV. The difference is due, of course, to the very different geomagnetic cutoffs at the two locations.

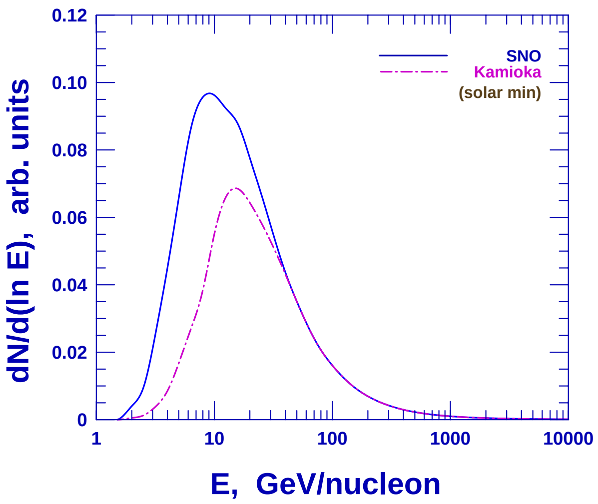

Figure 4. Cosmic ray response to sub–GeV neutrino events detected at Kamioka and Soudan 2/SNO at solar minimum.

The high geomagnetic cutoff at Kamioka will tend to mask the solar modulation of the cosmic ray flux. Table 1 shows the fraction of the interstellar flux that reaches us for modulation parameters Φ of 500 and 1000 MeV at several energies. These Φ values have been extracted from data by experiments that have measured the primary cosmic ray flux at solar minimum (Φ = 500 MeV) and solar maximum. The numbers in the Table are crude estimates assuming all cosmic ray nucleons are free protons. On the other hand, Φ values higher than 1000 MeV are expected at the true solar maximum.

Table 1
Effects of solar modulation. Columns 2&3 give flux decrease respective to the interstellar flux. Column 4 gives the ratio between the two.

Φ, MeV E, GeV	500	1000	max/min
5	0.63	0.41	0.65
10	0.79	0.64	0.81
15	0.86	0.74	0.86
20	0.89	0.80	0.90

An application of the values in Table 1 to the responses shown in Fig. 4 shows that the Soudan 2 & SNO neutrino fluxes will be affected by the solar modulation much more strongly than these at Kamioka. A study of these variations and a comparison of the effects at different geomagnetic locations will give us helpful hints for the importance of low energy cosmic rays for the production of neutrinos.

Such survey was done with data from the IMB experiment several years ago by the author with Bob Svoboda and John Learned. A very strong correlation of the sub–GeV neutrino events with the solar activity was observed. The correlation came out much too strong and our conclusion was that the solar modulation was overemphasized by instrumental effects.

5.2. Atmospheric muons.

Atmospheric muons and neutrinos have a common origin and it is thus natural to use the measured fluxes of atmospheric muons as a normalization of the neutrino predictions. This has been always done in the past, however a couple of years ago the muon fluxes measured throughout the atmosphere demonstrated clear deviations from 1D predictions. Muon fluxes seem to be reasonably well predicted at floating altitudes (4–5 g/cm^2) while the 1D calculated fluxes exceed the measured ones at low momenta and bigger atmospheric depths [24,25].

Subsequent calculations showed that the account for 3D effects are not less important for muons. The key here is not the shape of the production region, as in neutrino calculations,, but the correct account for the muon energy loss. An essential part of the 3D effects is also the bending of the muon trajectories in the geomagnetic field. 3D effects and muon bending increase the muon pathlength, energy loss and decay probability. While the effect on the muon fluxes is quite strong, the neutrino fluxes corrections are of second order, since the muons decay and generate neutrinos, possibly of slightly different energy.

Still, muon data make possible an important normalization. It requires, however, calculations accounting for all 3D effects, including the muon bending, and better studies of the experimental efficiency as a function of the muon angle and momentum. Because of the short duration of balloon flights the use of appropriate cosmic ray spectrum, if not measured by the same instrument, is very important.

6. CONCLUSIONS

The knowledge of the primary cosmic rays responsible for the bulk of the atmospheric neutrinos has significantly improved during recent years. To achieve the desired accuracy in the predictions one needs to correctly fold the solar modulation for the duration of the experiment. Comparisons of neutrino spectra at different geomagnetic locations and studies of muon spectra in the atmosphere and at sea level should also lead to improvements of our understanding of atmospheric neutrinos and to a better derivation of the oscillation parameters.

At higher energies, that are responsible for the neutrinos generating upward going muons, the cosmic rays spectrum is less known.

REFERENCES

1. J. Engel et al, Phys. Rev. D 46 (1992) 5013.
2. T.K. Gaisser & T. Stanev, Eur. Phys. J. C 15 (2000) 150.
3. W.R. Webber et al, Proc. 20th ICRC (Moscow) 1 (1987) 325.
4. E.-S. Seo et al. ApJ, 378 (1991) 763.
5. R. Belotti et al. Phys Rev. D60 (1999) 052002.
6. W. Menn et al. ApJ, 533 (2000) 281.
7. M. Boezio et al. ApJ, 518 (1999) 457.
8. J. Alcaraz et al. Phys. Lett. B490 (2000) 27.
9. J. Alcaraz et al. Phys. Lett. in print.
10. T. Sanuki et al. ApJ, in print.
11. V. Agrawal et al. Phys. Rev. D53 (1996) 1314; T.K. Gaisser & T. Stanev, Proc 24th ICRC (Rome) 1 (1995) 694.
12. K. Asakimori et al. ApJ, 502 (1998) 278.
13. A.V. Apanasenko et al. Proc. 26th ICRC (Salt Lake City) 3 (1999) 163.
14. L.J. Gleeson & W.I. Axford, ApJ, 154 (1968) 1011.
15. J. Chen & J.W. Bieber, ApJ, 405 (1993) 375.
16. see *http://nssdc.gsfc.nasa.gov/space/model/magnetos/igrf.html* for the International Geomagnetic Reference Field (IGRF) model.
17. P. Lipari, Astropart. Phys. 14 (2000) 153.
18. T. Futagami et al. Phys. Rev. Lett. 82 (1999) 5194.
19. P. Lipari, T.K. Gaisser & T. Stanev, Phys. Rev. D58 (1998) 073003.
20. P. Lipari, Astropart. Phys. 14 (2000) 171.
21. T. Kajita, these Proceedings.
22. G. Battistoni et al. Astropart. Phys. 12 (2000) 315.
23. G. Battistoni, these Proceedings.
24. M. Circella et al. Proc 25th ICRC (Durban) 7 (1997) 117.
25. M. Boezio et al. Phys. Rev. D62 (2000) 032007.